

# Lost-PLA Casting Process Development Using Material Extrusion with Low-Weight PLA

Mohammad Alshaikh Ali, Orkhan Huseynov, Ismail Fidan, and Fred Vondra

Tennessee Tech University  
Cookeville, TN 38505

## Abstract

The goal of this research is to develop a baseline procedure for lost-PLA casting process of aluminum. Traditional Manufacturing techniques and Smart Manufacturing techniques have their advantages and disadvantages. Integrating the traditional and modern aspects of manufacturing enhances the capabilities of manufacturing. In this study, low-weight PLA is used in a Material Extrusion (MEX) machine to fabricate sacrificial patterns for an aluminum lost-casting process. Different process parameters, after a calibration process, are tested for the MEX process. The MEX process parameters tested are: infill pattern, and top/bottom solid layers. The MEX process parameter investigation allows to draw conclusions to establish a standard for which parameters are ideal for the casting process. For this research, casting process parameters are set constant. The preliminary studies show that the lost-PLA casting process is successful in producing dimensionally accurate aluminum parts by a direct-pour casting process using the suggested MEX process parameters.

*Keywords:* Additive Manufacturing, Metal Casting, Fused Filament Fabrication, Material Extrusion, Investment Casting

## Introduction

Recent advances in AM technologies allow industries to fully utilize the potential of AM. While AM is an umbrella of versatile manufacturing technologies, the need for Traditional Manufacturing is still in high demand, due to the limitations of the relatively new manufacturing techniques [1]–[5]. Hybrid manufacturing is on the rise to overcome the limitations of manufacturing processes [6],[7]. An example of hybrid manufacturing would be to additively manufacture an object using Wire Arc technique and CNC machine the part afterwards. The Wire Arc technique can produce complex metal parts from a simple rod but has a rough surface finish. To overcome the surface roughness, a machining tool is used. This research explores a novel approach to implement another form of hybrid manufacturing: Lost-PLA Metal Casting (LPMC) which involves Material Extrusion (MEX) and metal casting.

Arguably the most used AM technique is MEX, shown in Figure 1, for its easy accessibility and low labor intensity compared to other AM technologies [8]–[10]. The MEX technique typically uses polymers as their medium which are extruded through a heated nozzle [11]. MEX's

popularity can also be attributed to the wide range of materials available that are tailored for use in MEX [12]–[15]. One of these materials is Polylactic Acid (PLA), which has been the main material to use for prototyping and some end-use applications [16]. While many PLA spools may have the same matrix material, manufacturers add additives to enhance different properties of the PLA [17],[18]. Some of these properties are printability, high temperature resistance, low density, surface quality, and several others. In this research, the focus is mainly on low-weight (LW) PLA from Colorfabb (colorfabb.com).

On the other end of the spectrum, metal casting has been practiced for over 5000 years [19]. Metal casting involves the pouring the molten into a mold. Depending on the casting process, the mold material would change. The most common and traditional type of metal casting is sand casting. In sand casting, the mold material is sand that takes the shape of a pattern. Traditionally, the patterns are fabricated from wood and are reusable. With sand casting, there comes a few limitations that are detrimental to some applications. An example of such limitations is that the pattern to be cast must not have a vertical surface but should be drafted with an angle that ranges from 5 to 15 degrees. This further implies that a pattern is not to have any negative draft nor overhangs.

To overcome these limitations, investment casting and lost-foam casting processes are used. The two casting processes are similar but not the same. Investment casting involves coating a sacrificial pattern, several times, with a coating that takes the shape of the pattern. Once the coating hardens, the coated pattern, traditionally made from wax, is then placed in a furnace that fully disintegrates the pattern material, leaving only the hard coating. Once the pattern is burned out, the coating is now a shell and molten metal can be poured into it. The molten metal takes the shape of the sacrificed pattern while being supported by the hardened coating. Lost-foam casting on the other hand, does not burn out the pattern beforehand. The pattern is made of polystyrene as opposed to wax and it disintegrates as the molten metal is poured into the mold.

Lost-foam casting and investment casting processes have major advantages over traditional sand casting, yet they are more labor intensive and costlier. Considering the low-cost manufacturing capability of MEX machines and the availability of a low-weight PLA medium, the authors consider the novel LPMC process.

To the extent of the authors' knowledge, LPMC has not been researched yet. On the contrary, investment casting using MEX and other AM techniques has been researched extensively for the sole purpose providing guidelines to the process and to manufacture parts used for other research objectives.

Carneiro et al. [20] used plaster molds to cast aluminum foam structures. The mold positives are made using SLA technology with meltable resin. The mold positive is then used in the plaster mold making process. Using a Voronoi algorithm, they were able to parametrize Computer Aided Design (CAD) models to achieve certain characteristics of the structures (Pores per inch or PPI). They had 5, 7, and 10 PPI designs. The designs are compared to commercially available metal foam structures. The authors were successful in casting their designs using the plaster mold.

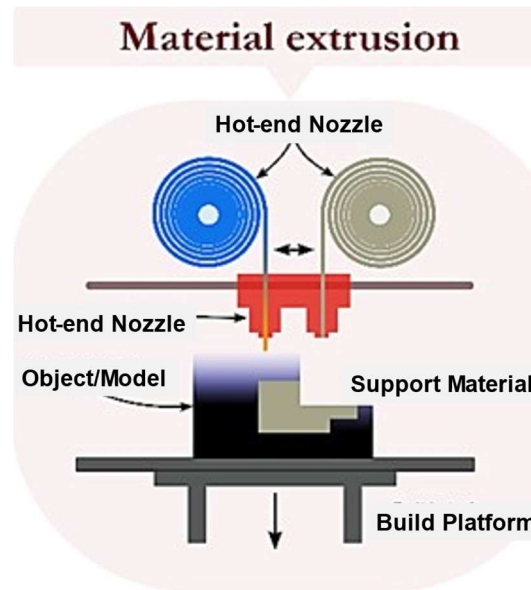


Figure 1: Material Extrusion (MEX) process shown in more detail [8]

They performed compression results on all 5 foam types, with 3 samples each. The designed foam exhibits twice the deformation energy absorption value of the commercial foam.

Almonti et al. [21] cast aluminum cellular structures based on PLA. Their MEX process parameters were 210 C for the nozzle temperature, 10 mm/s printing speed, and 0.2 mm layer height. The authors performed meso, macro, and microstructure analyses and compared the CAD model, the MEX-fabricated part, cast part. The authors discovered that most dimensional errors are introduced from the printed part. They claim that higher resolution stepper motors may improve the dimensional accuracy. They also found defects in the cast model along with some variations from the pattern, which is believed to be due to shrinkage and phase transitions.

### **MEX Basic Parameter Optimization**

The objective of this preliminary study is to establish a baseline for basic MEX process parameters, shown in Table 1 which include nozzle diameter, extrusion temperature, and extrusion multiplier, also known as flowrate percentage. The results from this study are used to draw conclusions for further testing and fabrication. In most cases, MEX materials need a few calibration models to establish the most dimensionally accurate settings. In this case, however, there is a foaming agent embedded in the PLA in order to allow for expansion. The expansion allows users to reduce flowrate in order to achieve the correct dimensions. With the decrease of flowrate, the part ends up being less dense than normal, due to the expanding foaming agent. For this reason, an extensive calibration process is needed to achieve the lowest weight with predictable dimensional error.

Table 1: Calibration DOE

Parameter	Value				
Nozzle Diameter (mm)	0.4		0.6		0.8
Nozzle Temperature (C)	225		235		245
Extrusion Multiplier (%)	100	70	50	40	35

The manufacturer of the LW-PLA claims the ability to print with 60% less density than normal PLA while retaining acceptable rigidity in the parts. The nozzle diameter was chosen as a process parameter since different size castings may be later investigated. Temperature and extrusion multiplier were chosen as per the manufacturer’s suggestion for calibration. The range for nozzle temperature is the median of what the manufacturer suggested. The extrusion multiplier range is descending range starting with 1.0 (100% flowrate) to see how the expansion agent reacts to the mixture of process parameters.

*MEX Setup*

The calibration tests utilized 20 mm cubes, shown in Figure 2, which are simply added from the included library with PrusaSlicer, which is the slicer used throughout this study. The cubes’ process parameters are then changed to have no top layers, no infill, and two walls. The investigated process parameters, shown in Table 2, are then changed to represent each combination of all process parameter levels. The cubes are fabricated one at a time on an unheated smooth PEI sheet with a thin layer of glue applied. The nozzle is switched only after all samples have been fabricated from the already installed nozzle.

*Weight and Dimension Measurement Setup*

The mass of the cubes is measured using a Mettler Toledo PL-602S [22] weight scale. This weight scale measures with an accuracy of up to a 100<sup>th</sup> of a gram, for the specimens will vary within that scale. Vernier calipers are used to measure overall dimensions of the cubes. The

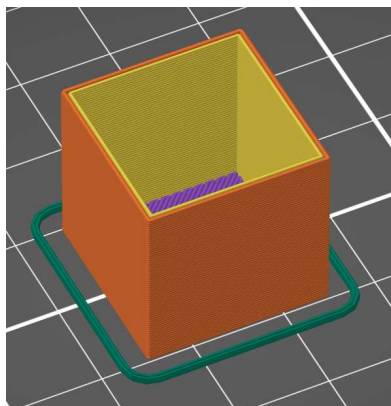


Figure 2: Sliced cube models used for calibration

measurements taken are of the overall x-axis, y-axis, and z-axis dimensions, in addition to the thickness of the walls. For wall measurements, four measurements are taken and averaged, due to the ununiform cooling that may alter at least one wall's dimensions. It should be noted that the wall extrusion width is not fixed, as it is optimized automatically based on the nozzle diameter.

### *Calibration Study Results*

Data collected is analyzed for the purpose of establishing a baseline for optimum dimensional accuracy and weight reduction. The resulting data indicates that with the increase of nozzle diameter, the average dimensional error increases. This leads to the conclusion that higher nozzle diameter cause more dimensional variation when exposed to different flowrates and temperatures. While this is a calibration study and error is expected, a high error average implies that calibration would not be controllable in an efficient manner.

A higher temperature should lead to a higher expansion rate of the foaming agent which should directly correlate with a higher dimensional error according to the manufacturer's specifications. In this study, different temperature ranges do not have a major effect on dimensional error, which is contrary to the manufacturer's suggestions. In fact, the 245 C temperature consistently produced the heaviest parts, on average. This is believed to be due to the lower viscosity as temperature increases.

Extrusion multiplier variations consistently result in a linear trend for weight and dimension measurements. Descending in flow causes a linear decrease in dimensions and weight. In addition, the weight reduction error is calculated, which is the error between the anticipated weight reduction and the actual weight reduction. For example, if the part weighs one gram at 100% flow, then it should weigh 0.35 grams with 35% flow. The lowest error indicates highest predictability when aiming for a certain weight, which can be quite helpful in future studies. The lowest weight reduction error is achieved by cubes fabricated with a 0.6 mm nozzle at 235 C, and 0.4 mm nozzle at 225 C. The averages for all errors are shown in Table 2.

*Table 2: Data averaged over all extrusion percentages*

<b>Parameter Value</b>	<b>Average Weight (g)</b>	<b>Average Dimensional Error (%)</b>	<b>Average Weight Error (%)</b>
<i>Nozzle Size (mm)</i>			
0.4	1.18	0.398	0.984
0.6	1.37	1.202	0.721
0.8	1.85	1.618	0.896
<i>Nozzle Temperature (C)</i>			
225	1.464	1.1	0.72
235	1.46	1.09	1.08
245	1.476	1.025	0.79

In order to decide which combination of parameter values is ideal for predictable casting patterns, the lowest weight and lowest overall errors should be considered. Based on results, 35% extrusion consistently produced the lightest parts, as expected, with relatively small overall errors. Of all the 35% extrusion parts, 0.6 mm diameter at 235 C and 0.4 mm diameter at 225 C parts stand out due to their low overall errors. It is well established that 0.6 mm nozzles are capable of producing parts significantly faster than the smaller nozzles, considering larger toolpaths, while maintaining a high level of detail if needed. For this reason, the ideal parameter value combination chosen for further studies is with a 0.6 mm nozzle diameter, 35% extrusion, and 235 C nozzle temperature.

### **Lost-PLA Metal Casting**

The previous section provided a baseline to start with for basic parameters with regards to least weight and highest dimensional accuracy. For further investigation on LPMC, a cuboid is utilized. The cuboid is imported from the slicer’s included library and scaled to have dimensions of 120x30x30 mm. Process parameters for MEX process are infill pattern, solid layers (top/bottom), and print orientation. The levels and their values are shown in Table 3. Three cuboids are fabricated at the same time with a nozzle temperature of 235 C, 0.035 flowrate, and a 0.6 mm nozzle diameter. In addition, a five-inch-tall sprue is fabricated and later glued to the part using a hot glue gun. The setups for MEX and other measurements are consistent with the calibration setup used previously.

#### *Casting Setup*

At this stage there are only a few controlled variables on the casting side. The metal used for casting is Aluminum which is consistently poured at 788 C. Different sand types are used to perform the LPMC process which include K-Bond and Mullite. K-Bond is typically used for traditional two-part mold castings, while mullite is used to support shells during investment and lost-foam casting. The general setup is demonstrated in Figure 3 and the sacrificial pattern model in Figure 4.

For the different sand types, different molding techniques are used yet the molds look similar as seen in Figure 5. K-bond required a tall two-part flask where the part is positioned upside down and sand is packed tightly around it until the flask is filled with sand. Once the flask is filled, the flask is transported to the pouring station and positioned right side up. The mold is now ready to have molten aluminum poured into it.

*Table 3: MEX parameters to be tested*

<b>Pattern Type</b>	<b>Solid Layers</b>
Gyroid	5
Support Cubic	
Lightning	7

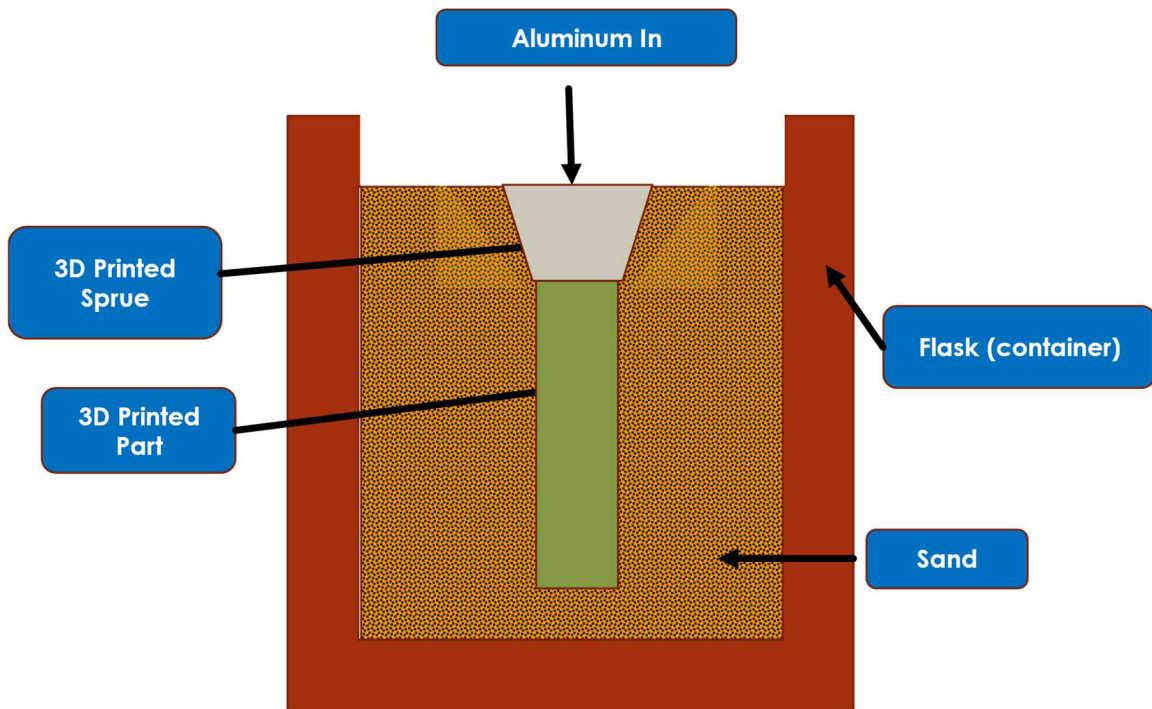


*Figure 3: General casting setup diagram*

For the Mullite sand, a much faster process is employed. A barrel is filled with Mullite sand to an appropriate level based on the height of the sacrificial part. The barrel is then placed on a vibrating platform, whose control box is shown in Figure 6. The platform operates on a high and low setting which corresponds to the vibration magnitude. The barrel is vibrated at the high setting initially while gently pushing the sacrificial pattern into the sand. Once the pattern reaches the desired depth, the platform is switched to vibrate at the low setting. The low setting does not allow the pattern to be pushed further but allows the sand to tightly settle for pouring. The barrel is then transferred to the pouring station. Before pouring molten aluminum, compressed air is used to blow out any sand that fell in the sprue.

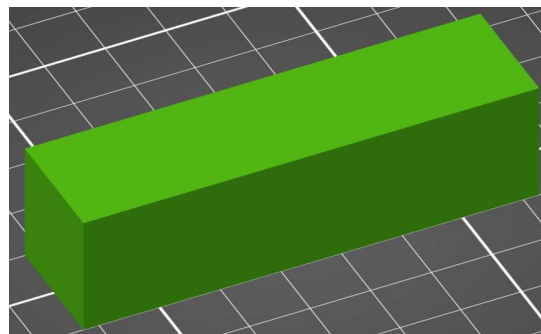


*Figure 4: Cuboid model used for casting*

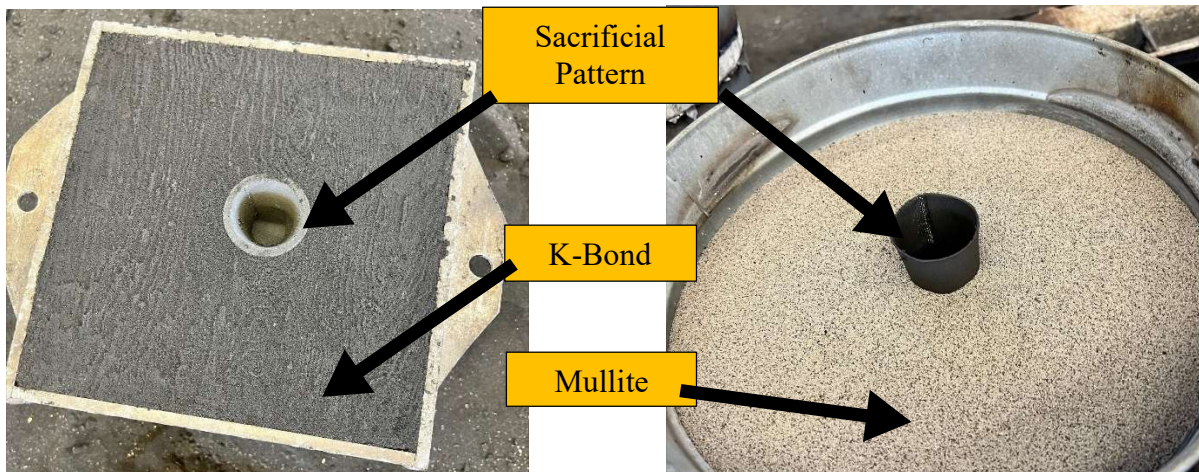


Figure 5: Ready-to-pour setups for both sand types

After pouring, the parts are allowed to solidify 15-20 minutes, and then removed from the molds to be air-cooled. The sprue is then cut off using a band saw and the aluminum cuboids are then wire-brushed to get rid of any leftover sand. To measure the dimensions of the aluminum cuboids, vernier calipers are used. Some parts are milled and sanded as the band saw does not precisely cut the sprue off. Due to some parts experiencing rough surfaces, a vice is used to clamp the part tightly, and then measurements are taken of the distance between the two grips of the vice. This ensures the calipers are not giving isolated and unrepresentative measurements, since the calipers are sensitive to rough surfaces.

### *Process Discussion*

Casting with both methods yields successful casts that closely represent the sacrificial cuboids. There are few considerations to take into account despite the success in casting. The mold-making process using K-Bond sand takes approximately 30 minutes, depending on the user, and moderate effort to pack sand tightly around the sacrificial pattern while holding the pattern down. The process with Mullite on the other hand takes five minutes or less. The mullite process uses a vibration platform which accelerates the process of mold making.



*Figure 6: Vibration platform control box*

The last and most important aspect to consider is the safety and reliability of each sand type undergoing LPMC. As mentioned previously, the larger grain allows gases generated by the evaporation of PLA to escape from within the mold. The finer grain sand, K-Bond, does not allow gases to escape as easily. For this reason, it is observed that at the beginning of pouring molten aluminum, the gases generated push back on the inlet and generates some backsplash of molten aluminum. This backsplash can be extremely dangerous and therefore should be avoided. While there is some push back from the larger grain, Mullite, the head pressure is enough to force the gases to escape from within the mold instead.

#### *Casting Results Discussion*

Another important aspect to observe is the surface roughness of the casts. The K-Bond is a much finer grain of sand than Mullite since K-Bond does not have to be permeable. Mullite on the other hand must be permeable in order to allow gases to escape. The larger grain expectedly yields a much rougher surface than the smaller grain. With that said, both sand types yielded workable successful casts, as seen in Figure 7.

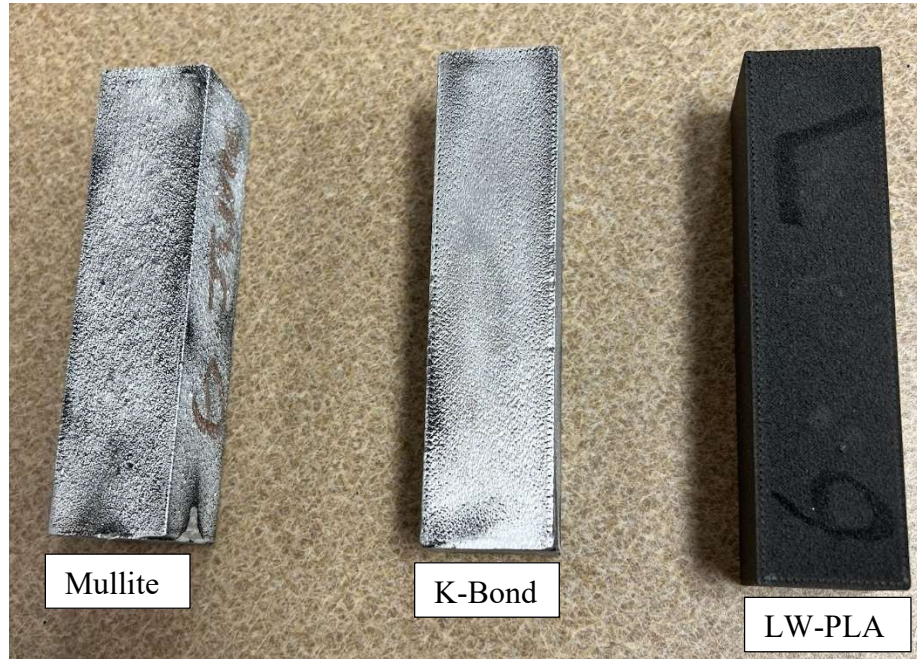


*Figure 7: Cast parts and pattern comparison*

The AM process parameters investigated in this study provided preliminary information on the effect they have on casting results. With that said, the results indicate that a few parameter values should not be considered for future studies. Looking at Figure 8, the defects are only seen in parts from patterns printed with gyroid infill. Considering all parts were cast in a random order and not in specific batches, the pouring variability is eliminated and leaves the gyroid infill pattern to be the common denominator in their defects. As for pattern type on shrinkage, gyroid filled patterns produced casts with the least shrinkage, followed by lightning and support cubic, respectively, as seen in Table 4. The gyroid is not considered, however, to be a good pattern to have due to the defects mentioned previously.

This leaves lightning and support cubic to be considered as the optimum infill pattern for future studies. The standard deviation is lowest for support cubic which indicates higher repeatability with support cubic rather than lightning. It should also be noted that due to the nature of the material used, lightning infill provided very little internal support to the part, which

*Table 4: Simple statistics for infill pattern effect on shrinkage*

<b>Pattern Type</b>	<b>Average Shrinkage (%)</b>	<b>Standard Deviation</b>
Gyroid	-0.222	0.801
Support Cubic	-0.627	0.206
Lightning	-0.479	0.601

caused the printed parts to have an apparent seam along the long edge of the part (x-axis). This seam is believed to be caused by the higher residual stresses that are produced in solid layers compared to the shells.

Finally looking at solid layers effect on average shrinkage percentage, Figure 9 indicates that the slight increase in solid layers does not have an effect on the shrinkage of cast parts. It is obvious that lower count of solid layers would be less resistant to evaporation thus increasing process efficiency. However, a lower number of solid layers, especially top layers, is usually impractical and leads to void-filled, bumpy, and potentially failed parts. For this reason, five top layers are chosen as the optimum solid layer count to be used in future studies using the LPMC process.



*Figure 8: Defects shown in parts cast from gyroid-filled patterns*



## Acknowledgements

This study is supported by the Department of Manufacturing and Engineering Technology at Tennessee Technological University.

## References

- [1] S. Hasanov, A. Gupta, F. Alifui-Segbaya, and I. Fidan, "Hierarchical homogenization and experimental evaluation of functionally graded materials manufactured by the fused filament fabrication process," *Compos Struct*, vol. 275, Nov. 2021, doi: 10.1016/J.COMPSTRUCT.2021.114488.
- [2] S. Hasanov *et al.*, "Review on Additive Manufacturing of Multi-Material Parts: Progress and Challenges," *Journal of Manufacturing and Materials Processing*, vol. 6, no. 1, p. 4, Dec. 2021, doi: 10.3390/jmmp6010004.
- [3] A. Gupta, S. Hasanov, I. Fidan, and Z. Zhang, "Homogenized modeling approach for effective property prediction of 3D-printed short fibers reinforced polymer matrix composite material," *The International Journal of Advanced Manufacturing Technology*, vol. 118, no. 11–12, pp. 4161–4178, Feb. 2022, doi: 10.1007/s00170-021-08230-9.
- [4] H. Si, Z. Zhang, O. Huseynov, I. Fidan, S. R. Hasan, and M. Mahmoud, "Machine Learning-Based Investigation of the 3D Printer Cooling Effect on Print Quality in Fused Filament Fabrication: A Cybersecurity Perspective," *Inventions*, vol. 8, no. 1, p. 24, Jan. 2023, doi: 10.3390/inventions8010024.
- [5] M. Mohammadzadeh and I. Fidan, "Tensile Performance of 3D-Printed Continuous Fiber-Reinforced Nylon Composites," *Journal of Manufacturing and Materials Processing*, vol. 5, no. 3, p. 68, Jun. 2021, doi: 10.3390/jmmp5030068.
- [6] J. Watson, F. Vondra, and I. Fidan, "The Development of a Framework for 3D Printing, Casting, and Entrepreneurship," in *2017 ASEE Annual Conference & Exposition Proceedings*, ASEE Conferences. doi: 10.18260/1-2--28955.
- [7] T. Fresques, D. Cantrell, and I. Fidan, "The development of a framework between the 3D printed patterns and sand-cast work pieces," *International Journal of Rapid Manufacturing*, vol. 5, no. 2, p. 170, 2015, doi: 10.1504/IJRAPIDM.2015.073575.
- [8] A. Gupta, S. Hasanov, and I. Fidan, "Thermal characterization of short carbon fiber reinforced high temperature polymer material produced using the fused filament fabrication process," *J Manuf Process*, vol. 80, pp. 515–528, Aug. 2022, doi: 10.1016/J.JMAPRO.2022.06.024.
- [9] M. Alshaikh Ali and I. Fidan, "Benchmarking Studies on Energy Usage and Lattice Infill Pattern for Common Additive Manufacturing Technologies," Ann Arbor, 2022. [Online]. Available: <https://ezproxy.tntech.edu/login?url=https://www.proquest.com/dissertations-theses/benchmarking-studies-on-energy-usage-lattice/docview/2701023448/se-2?accountid=28833>
- [10] I. Fidan *et al.*, "Recent Inventions in Additive Manufacturing: Holistic Review," *Inventions*, vol. 8, no. 4, p. 103, Aug. 2023, doi: 10.3390/inventions8040103.
- [11] M. Alshaikh Ali, I. Fidan, and K. Tantawi, "Investigation of the impact of power consumption, surface roughness, and part complexity in stereolithography and fused

- filament fabrication,” *The International Journal of Advanced Manufacturing Technology*, vol. 126, no. 5–6, pp. 2665–2676, May 2023, doi: 10.1007/s00170-023-11279-3.
- [12] O. Huseynov, S. Hasanov, and I. Fidan, “Influence of the matrix material on the thermal properties of the short carbon fiber reinforced polymer composites manufactured by material extrusion,” *J Manuf Process*, vol. 92, pp. 521–533, Apr. 2023, doi: 10.1016/j.jmapro.2023.02.055.
- [13] A. R. Zanjanijam, I. Major, J. G. Lyons, U. Lafont, and D. M. Devine, “Fused Filament Fabrication of PEEK: A Review of Process-Structure-Property Relationships,” *Polymers (Basel)*, vol. 12, no. 8, p. 1665, Jul. 2020, doi: 10.3390/polym12081665.
- [14] E. Manzo, N. Downey, P. Cheetham, and S. Pamidi, “Fabrication and Characterization of Additively Manufactured Electrical Insulation System Components Using SLA and FDM Printers,” in *2022 IEEE Electrical Insulation Conference (EIC)*, IEEE, Jun. 2022, pp. 69–72. doi: 10.1109/EIC51169.2022.9833172.
- [15] J. Ryan *et al.*, “Post-Processing of 3D-Printed Polymers,” *Technologies 2021, Vol. 9, Page 61*, vol. 9, no. 3, p. 61, Aug. 2021, doi: 10.3390/TECHNOLOGIES9030061.
- [16] S. Hasanov *et al.*, “Review on Additive Manufacturing of Multi-Material Parts: Progress and Challenges,” *Journal of Manufacturing and Materials Processing*, vol. 6, no. 1, p. 4, Dec. 2021, doi: 10.3390/jmmp6010004.
- [17] A. Gupta, S. Hasanov, and I. Fidan, “Thermal characterization of short carbon fiber reinforced high temperature polymer material produced using the fused filament fabrication process,” *J Manuf Process*, vol. 80, pp. 515–528, Aug. 2022, doi: 10.1016/j.jmapro.2022.06.024.
- [18] A. Nasirov, A. Gupta, S. Hasanov, and I. Fidan, “Three-scale asymptotic homogenization of short fiber reinforced additively manufactured polymer composites,” *Compos B Eng*, vol. 202, p. 108269, Dec. 2020, doi: 10.1016/j.compositesb.2020.108269.
- [19] “A Brief History of Metal Casting • Bernier Metals.” <https://bernierinc.com/brief-history-metal-casting/> (accessed Jun. 30, 2023).
- [20] V. H. Carneiro, S. D. Rawson, H. Puga, and P. J. Withers, “Macro-, meso- and microstructural characterization of metallic lattice structures manufactured by additive manufacturing assisted investment casting,” *Sci Rep*, vol. 11, no. 1, Dec. 2021, doi: 10.1038/s41598-021-84524-y.
- [21] D. Almonti, G. Baiocco, V. Tagliaferri, and N. Ucciardello, “Design and Mechanical Characterization of Voronoi Structures Manufactured by Indirect Additive Manufacturing,” *Materials*, vol. 13, no. 5, Mar. 2020, doi: 10.3390/MA13051085.
- [22] Mettler Toledo, “PL602-s [https://www.mt.com/my/en/home/products/Laboratory\\_Weighing\\_Solutions/Precision\\_Balances/Standard/PL-E\\_Precision/PL602E.html](https://www.mt.com/my/en/home/products/Laboratory_Weighing_Solutions/Precision_Balances/Standard/PL-E_Precision/PL602E.html), accessed on 07/01/2023.”